



# Asymmetric division triggers cell-specific gene expression through coupled capture and stabilization of a phosphatase

## Citation

Bradshaw, Niels, and Richard Losick. 2015. "Asymmetric division triggers cell-specific gene expression through coupled capture and stabilization of a phosphatase." *eLife* 4 (1): e08145. doi:10.7554/eLife.08145. <http://dx.doi.org/10.7554/eLife.08145>.

## Published Version

doi:10.7554/eLife.08145

## Permanent link

<http://nrs.harvard.edu/urn-3:HUL.InstRepos:24984022>

## Terms of Use

This article was downloaded from Harvard University's DASH repository, and is made available under the terms and conditions applicable to Other Posted Material, as set forth at <http://nrs.harvard.edu/urn-3:HUL.InstRepos:dash.current.terms-of-use#LAA>

## Share Your Story

The Harvard community has made this article openly available.  
Please share how this access benefits you. [Submit a story](#).

[Accessibility](#)

# Asymmetric division triggers cell-specific gene expression through coupled capture and stabilization of a phosphatase

Niels Bradshaw, Richard Losick\*

Department of Molecular and Cellular Biology, Harvard University, Cambridge, United States

**Abstract** Formation of a division septum near a randomly chosen pole during sporulation in *Bacillus subtilis* creates unequal sized daughter cells with dissimilar programs of gene expression. An unanswered question is how polar septation activates a transcription factor ( $\sigma^F$ ) selectively in the small cell. We present evidence that the upstream regulator of  $\sigma^F$ , the phosphatase SpoII $\epsilon$ , is compartmentalized in the small cell by transfer from the polar septum to the adjacent cell pole where SpoII $\epsilon$  is protected from proteolysis and activated. Polar recognition, protection from proteolysis, and stimulation of phosphatase activity are linked to oligomerization of SpoII $\epsilon$ . This mechanism for initiating cell-specific gene expression is independent of additional sporulation proteins; vegetative cells engineered to divide near a pole sequester SpoII $\epsilon$  and activate  $\sigma^F$  in small cells. Thus, a simple model explains how SpoII $\epsilon$  responds to a stochastically-generated cue to activate  $\sigma^F$  at the right time and in the right place.

DOI:10.7554/eLife.08145.001

## Introduction

How genetically identical daughter cells adopt dissimilar programs of gene expression following cell division is a fundamental problem in developmental biology. A common mechanism for establishing cell-specific gene expression is asymmetric segregation of a cell fate determinant between the daughter cells (Horvitz and Herskowitz, 1992; Neumüller and Knoblich, 2009). In polarized cells, intrinsic asymmetry can be inherited from generation to generation. For example, the dimorphic bacterium *Caulobacter crescentus* localizes certain cell fate determinants to the old cell pole, leading to their asymmetric distribution following division (Iniesta and Shapiro, 2008; Bowman et al., 2011). However, non-polarized cells such as *Bacillus subtilis* must generate asymmetry de novo, which is passed on to the daughter cells to differentiate.

*Bacillus subtilis* divides by binary fission to produce identical daughter cells during vegetative growth but switches to asymmetric division when undergoing the developmental process of spore formation (Piggot and Coote, 1976; Stragier and Losick, 1996). To sporulate, cells place a division septum near a randomly chosen pole of the cell (Veening et al., 2008) to create two unequally sized daughter cells with dissimilar programs of gene expression. The smaller cell, the forespore, which largely consists of the cell pole, will become the spore, whereas the larger cell, the mother cell, nurtures the developing spore (Figure 1B). An enduring mystery of this developmental system is how stochastically generated asymmetry initiates dissimilar programs of gene expression in the daughter cells resulting from polar division (Barak and Wilkinson, 2005).

The earliest acting cell-specific regulatory protein in the sporulation program is the transcription factor  $\sigma^F$ . The  $\sigma^F$  factor and the proteins that control it – SpoIIAB, SpoIIAA, and SpoII $\epsilon$  – are produced at the onset of sporulation (Gholamhoseinian and Piggot, 1989), but  $\sigma^F$  is held inactive until the completion of asymmetric cell division, when it turns on gene expression selectively in the

\*For correspondence: losick@mcb.harvard.edu

Competing interest: See page 16

Funding: See page 16

Received: 16 April 2015

Accepted: 13 October 2015

Published: 14 October 2015

Reviewing editor: Michael Laub, Massachusetts Institute of Technology, United States

© Copyright Bradshaw and Losick. This article is distributed under the terms of the Creative Commons Attribution License, which permits unrestricted use and redistribution provided that the original author and source are credited.

**eLife digest** An important question in biology is how genetically identical cells activate different sets of genes. This is particularly perplexing for cells that rely on random events to specify the genes they switch on. Normally, cells of a bacterium called *Bacillus subtilis* divide symmetrically to produce two identical cells that express identical sets of genes. However, *B. subtilis* cells can also undergo a developmental program to form a spore to help it survive periods of extreme conditions. To do this, first a *B. subtilis* cell divides asymmetrically by placing the site of division close to a randomly selected end of the cell. This creates a smaller cell that becomes the spore and a larger cell that nurtures the developing spore. Each cell must turn on different genes to play its role in spore development, but how asymmetry in the position of cell division leads to these differences in gene expression has been a longstanding mystery.

Bradshaw and Losick studied a regulatory protein called SpoII $\epsilon$ , which is responsible for switching on genes in the small cell. SpoII $\epsilon$  is made before cells divide asymmetrically, but only accumulates in the small cell. The experiments revealed that an enzyme broke down the SpoII $\epsilon$  protein if it wasn't in the small cell. This prevented SpoII $\epsilon$  from incorrectly switching on genes before division was completed or in the large cell.

Protection of SpoII $\epsilon$  from being broken down in the small cells was then shown to be linked to the placement of cell division; SpoII $\epsilon$  first accumulates at the asymmetrically positioned cell division machinery and then is transferred to a secondary binding site at the nearby end of the cell. Capture of SpoII $\epsilon$  at the end of the cell was coupled to its stabilization as SpoII $\epsilon$  molecules interacted with one another to form large complexes.

Together these findings provide a simple mechanism to link the asymmetric position of cell division to differences in gene expression. Future studies will focus on understanding how SpoII $\epsilon$  is captured at the end of the cell and how this prevents SpoII $\epsilon$  from being degraded.

DOI:10.7554/eLife.08145.002

forespore (Margolis *et al.*, 1991; Stragier and Losick, 1996) (Figure 1A,B). SpoIIAB is an anti-sigma factor that traps  $\sigma^F$  in an inactive complex (Min *et al.*, 1993; Duncan and Losick, 1993). Escape from SpoIIAB is mediated by the anti-anti-sigma factor SpoIIAA (Diederich *et al.*, 1994). SpoIIAA is, in turn, activated by SpoII $\epsilon$ , a member of the PP2C family of protein phosphatases (Bork *et al.*, 1996; Levnikov *et al.*, 2011). SpoII $\epsilon$  converts the inactive phosphorylated form of SpoIIAA (SpoIIAA-P) to the active dephosphorylated form (Duncan *et al.*, 1995) (Figure 1A). Dephosphorylation of SpoIIAA-P by SpoII $\epsilon$  is therefore the critical event in activating  $\sigma^F$ . Understanding how SpoII $\epsilon$  reads out cellular cues to delay dephosphorylation of SpoIIAA-P until after septation and restrict phosphatase activity to the forespore is thus the central challenge in understanding how cell-specific gene transcription is established during sporulation.

SpoII $\epsilon$  consists of three domains: a PP2C phosphatase domain at the C-terminus, a ten-pass transmembrane domain at the N-terminus, and a 270-amino acid central domain (henceforth referred to as the regulatory domain) that is important for regulating SpoII $\epsilon$  compartmentalization and activity (Figure 2B; Arigoni *et al.*, 1999). Prior to asymmetric cell division, SpoII $\epsilon$  localizes to the polar divisome and contributes to its placement (Arigoni *et al.*, 1995; Ben-Yehuda and Losick, 2002). After septation is complete, SpoII $\epsilon$  is found principally in the forespore and to a limited extent at a second polar divisome near the distal cell pole (Figure 1C, Video 1).

Here we describe three interdependent features of SpoII $\epsilon$  that together explain how SpoII $\epsilon$  links polar septation to the cell-specific activation of  $\sigma^F$ : (1) SpoII $\epsilon$  is proteolytically unstable and is degraded dependent on the AAA+ protease FtsH; (2) SpoII $\epsilon$  is transferred from the polar divisome – the de novo origin of asymmetry – to the proximal cell pole during polar septation; and (3) SpoII $\epsilon$  forms homooligomeric complexes which promote capture at the pole, protection from proteolysis and activation as a phosphatase, thus linking the cues that direct localization of SpoII $\epsilon$  to its stabilization and activation.

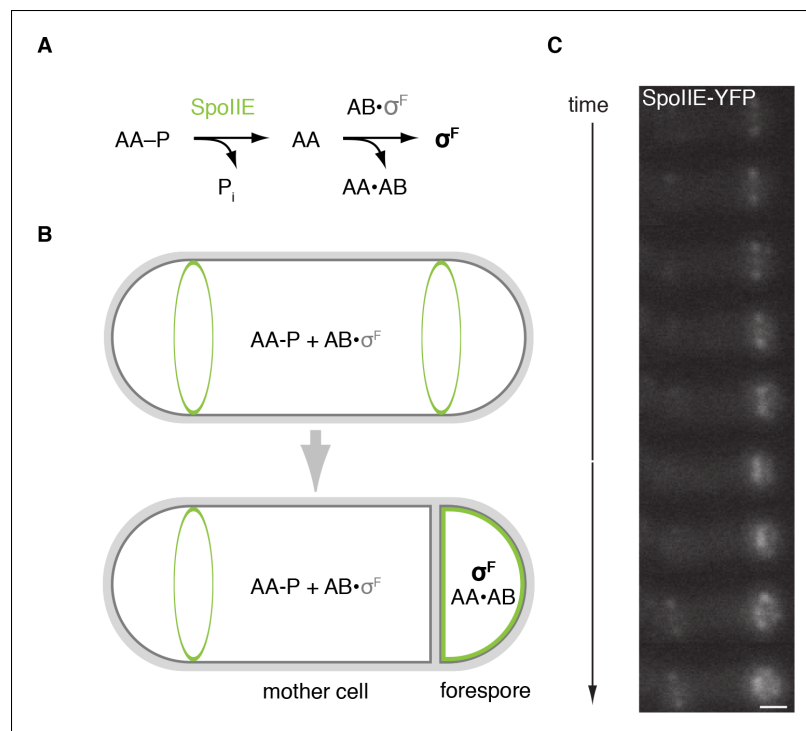


**Figure 1.** SpolIE is compartmentalized in the forespore and activates  $\sigma^F$ . (A) Diagram of the pathway for  $\sigma^F$  activation. Phosphorylated SpoIIAA (AA-P) is dephosphorylated by SpolIE. Dephosphorylated SpoIIAA (AA) then binds to SpoIIAB (AB) displacing  $\sigma^F$  and leading to  $\sigma^F$ -directed transcription. (B) SpolIE (green), AA, AB and  $\sigma^F$  are produced in predivisional cells. Prior to completion of asymmetric cell division SpolIE associates with the polar divisome near one or both cell poles (the pole at which division initiates is chosen randomly). Following completion of cytokinesis, SpolIE is enriched in the forespore where it dephosphorylates AA-P to activate  $\sigma^F$ . (C) A montage of images taken every 6 min from a single sporulating cell (strain RL5876) producing SpolIE-YFP. Cells are oriented with the forespore on the right as in the diagram. A movie of this sporulating cell is provided as **Video 1**. Scale bar: 0.5  $\mu\text{m}$ .

DOI: [10.7554/eLife.08145.003](https://doi.org/10.7554/eLife.08145.003)

The following figure supplements are available for Figure 1:

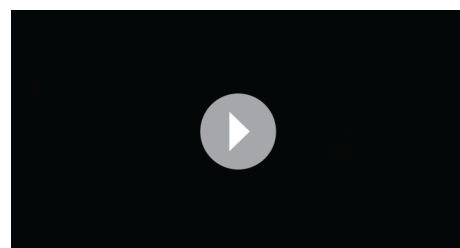
**Figure supplement 1.** SpolIE constricts along with FtsZ during asymmetric cell division.

DOI: [10.7554/eLife.08145.004](https://doi.org/10.7554/eLife.08145.004)

## Results

### SpolIE is degraded in an FtsH-dependent manner

Although transcription of *spoIIIE* commences in pre-divisional cells and continues in the mother cell following cytokinesis (Fujita and Losick, 2003), SpolIE protein and activity are restricted to the forespore (Figure 2A). This apparent contradiction led us to consider the possibility that spatially



**Video 1.** Movie file of the sporulating cell shown in Figure 1C (2fps).

DOI: [10.7554/eLife.08145.005](https://doi.org/10.7554/eLife.08145.005)

restricted proteolysis contributes to compartmentalization of SpolIE. Selective stabilization of SpolIE in the forespore coupled to efficient global degradation would enrich SpolIE in the forespore despite ongoing transcription of *spoIIIE* in predivisional cells and the mother cell. To investigate this hypothesis, we sought to determine if SpolIE turns over on a timescale commensurate with  $\sigma^F$  activation and, if so, to identify the responsible protease.

To detect SpolIE degradation during sporulation, we monitored the disappearance of SpolIE

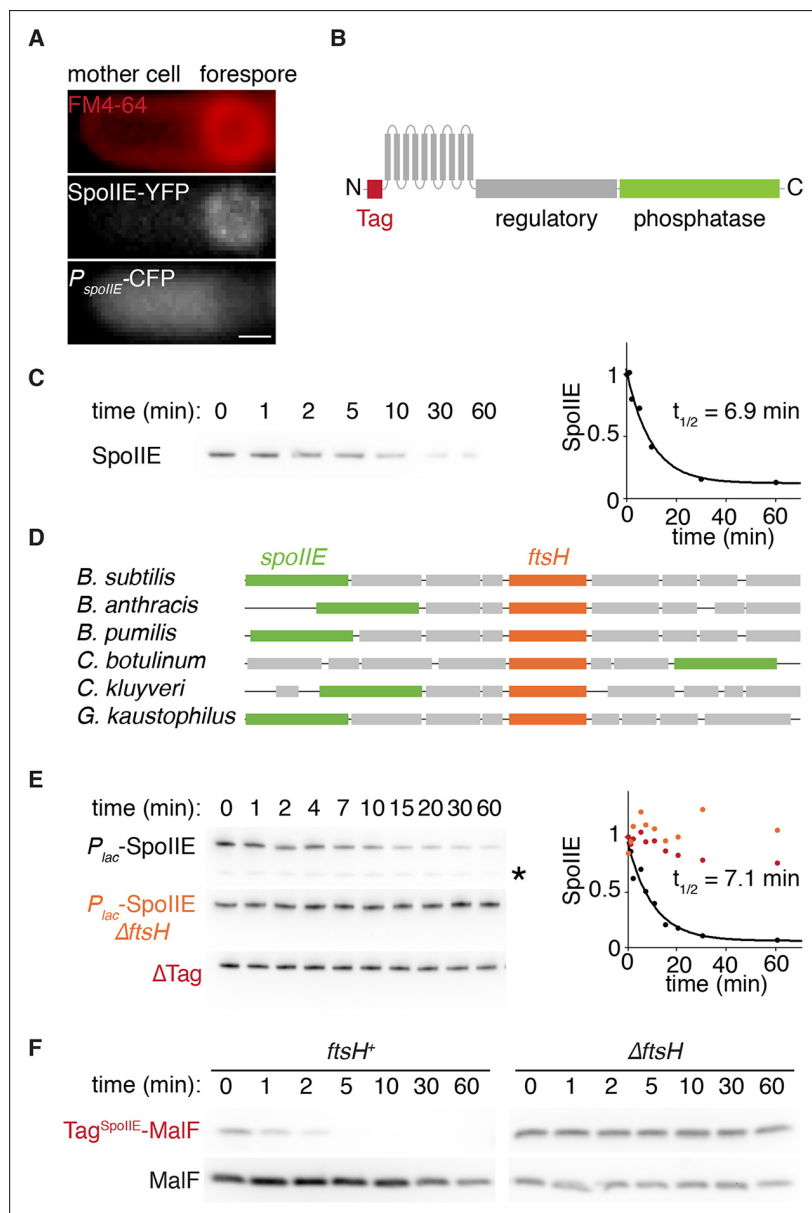


**Figure 2.** SpoII degradation depends on FtsH. (A) SpoII is compartmentalized to the forespore. A single sporulating cell (strain RL5874) is shown following the completion of asymmetric septation. The membrane stained with FM4-64 is shown in red above SpoII-YFP and CFP driven by an in frame fusion to the start of the *spoII* open reading frame. Scale bar: 0.5  $\mu$ m. (B) The domain architecture of SpoII. The N-terminal cytoplasmic tail (red), followed by 10 transmembrane-spanning segments, the regulatory region (amino acids 320–589, gray), and the phosphatase domain (amino acids 590–827, green). (C) SpoII is degraded during sporulation. Translation was arrested (by addition of 100  $\mu$ g/ml chloramphenicol) in sporulating cells producing SpoII-FLAG (strain RL5877), and samples were withdrawn at the indicated times. SpoII was detected by western blot using  $\alpha$ -FLAG monoclonal antibody (left). Quantitation of the western (right) fit to a single exponential equation. (D) The genes for *spoII* and *ftsH* are near each other in the genome with conserved synteny. The diagram shows genomic organization of diverse endospore forming species. Filled boxes indicate genes with *spoII* in green, *ftsH* in orange, and other genes in gray. (E) SpoII degradation requires FtsH, and FtsH mediated degradation requires the N-terminal cytoplasmic tail (Tag<sup>SpoII</sup>) of SpoII. Translation was arrested in vegetatively growing cells producing SpoII-FLAG with an IPTG inducible promoter (strain RL5878 wt, RL5879  $\Delta ftsH$ , and RL5880 SpoII- $\Delta$ Tag (residues 11–37 were deleted). Degradation was monitored (left) and quantitated (right) as in panel C. (F) Tag<sup>SpoII</sup> is sufficient to target a heterologous protein for FtsH-dependent degradation. Degradation of MalF-TM-FLAG fused at the N-terminus to either Tag<sup>SpoII</sup> (wt RL5888,  $\Delta ftsH$  RL5889) or the first 10 amino acids of SpoII (wt RL5890,  $\Delta ftsH$  RL5891) produced during exponential growth was monitored as in panel C.

DOI: [10.7554/eLife.08145.006](https://doi.org/10.7554/eLife.08145.006)

The following figure supplements are available for Figure 2:

**Figure supplement 1.** SpoII degradation depends on FtsH.

DOI: [10.7554/eLife.08145.007](https://doi.org/10.7554/eLife.08145.007)

with a C-terminal FLAG tag following inhibition of translation with chloramphenicol (**Figure 2C**). SpoII-FLAG was degraded with a half-life of 7 min, demonstrating that SpoII is unstable relative to the approximately 1 hr progression of asymmetric cell division and  $\sigma^F$  activation (**Figure 1C**) and supporting spatially restricted degradation as a plausible mechanism to compartmentalize SpoII.

Next, we sought to identify the protease that degrades SpoII. We noticed that the gene (*ftsH*) for the transmembrane AAA+ protease FtsH is located near *spoII* in the genome with highly conserved synteny (**Figure 2D**). Furthermore, FtsH is known to degrade transmembrane protein substrates (**Akiyama, 2009**), making it an attractive candidate protease for SpoII. FtsH degrades several proteins that block entry into sporulation and prevent the expression of *spoII*, such as the Spo0A inhibitor Spo0E (**Le and Schumann, 2009**). We therefore engineered the synthesis of SpoII during vegetative growth to bypass the requirement for FtsH in the expression of *spoII*. In exponential phase cells deleted for *ftsH*, SpoII was stable for more than 1 hr after chloramphenicol treatment, whereas in *ftsH* cells SpoII was degraded as rapidly as during sporulation ( $t_{1/2} = 7.1$  min) (**Figure 2E**). (SpoII instability and its dependence on FtsH was also seen with untagged SpoII [**Figure 2—figure supplement 1A,B**]). We conclude that SpoII is degraded in an FtsH-dependent manner. The simplest explanation for this is that SpoII is a direct substrate for the protease.

Finally, we attempted to identify the feature or features of SpoII that renders it susceptible to proteolysis by FtsH. Truncation of the N-terminal, cytosolic tail of SpoII (removal of residues 11 to 37) blocked degradation (**Figure 2E**,  $\Delta$ Tag), whereas removal of the regulatory domain or the phosphatase domain or substitution of the transmembrane domain with the first two transmembrane segments of *E. coli* MalF (MalF-TM) did not impede FtsH-dependent degradation (**Figure 2—figure supplement 1C**). Additionally, the first 37 amino acids of SpoII (Tag<sup>SpoII</sup>) were sufficient to confer FtsH-dependent degradation on a heterologous protein, MalF-TM-FLAG (**Figure 2F**). Therefore, the N-terminal tail of SpoII is a tag that is both necessary and sufficient for FtsH-dependent proteolysis.

## Degradation restricts SpoII and $\sigma^F$ activity to the forespore

To test whether SpoII degradation is required for compartmentalization of  $\sigma^F$  activity and SpoII, we examined the effect of blocking degradation during sporulation. Here and in the experiments that follow, we removed Tag<sup>SpoII</sup> from SpoII in cells that were wild type for *ftsH* to selectively block SpoII degradation and circumvent off-target effects from other FtsH substrates had we used an *ftsH* mutation. Indeed, we observed a dramatic increase in aberrant activation of  $\sigma^F$  in  $\Delta$ tag *spoII* cells (**Figure 3A**). Whereas in wild-type cells  $\sigma^F$  activity was highly specific for the forespore (less than 2% non-specific activation),  $\Delta$ tag *spoII* caused non-specific activation of  $\sigma^F$  in 71% of the cells (**Figure 3B**). Quantification of  $\sigma^F$  activity with a *lacZ* reporter revealed that a strain with  $\Delta$ tag *spoII* activated  $\sigma^F$  with a similar time dependence but had 10-fold elevated  $\sigma^F$  activity (**Figure 3C**).

Activation of  $\sigma^F$  is tightly coupled to the completion of asymmetric cell division, and SpoII mutants have been characterized that uncouple cell division and  $\sigma^F$  activation (**Carniol et al., 2004; Feucht, et al., 2002; Hilbert and Piggot, 2003**). In contrast to these other cases of  $\sigma^F$  mis-activation in predivisional cells, stabilization of SpoII led to activation of  $\sigma^F$  primarily in cells that had completed asymmetric cell division (**Figure 3A,D**). Thus, stabilization of SpoII only partially uncouples  $\sigma^F$  activation from cell division.

Consistent with the idea that degradation contributes to compartmentalization of  $\sigma^F$  activity by helping to restrict SpoII to the forespore, we observed a striking correlation between elevated levels of  $\Delta$ Tag-SpoII in the mother cell and mis-activation of  $\sigma^F$  (**Figure 3A** bottom panels). Together, these data indicate that SpoII degradation is required for compartmentalization both of SpoII and  $\sigma^F$  activity.

## SpoII mutants blocked in compartmentalization and $\sigma^F$ activation

How is SpoII selectively stabilized in the forespore? We considered two models: (1) FtsH is not active in the forespore, or (2) specific features of SpoII stabilize it in the forespore. To test the former possibility, we engineered the production of the model FtsH substrate Tag<sup>SpoII</sup>-MalF using a forespore specific,  $\sigma^F$ -dependent promoter. Tag<sup>SpoII</sup>-MalF was rapidly degraded in a manner dependent on the Tag<sup>SpoII</sup> (**Figure 3—figure supplement 1**). Therefore FtsH is active in the forespore, suggesting that SpoII is specifically stabilized against FtsH-dependent degradation.



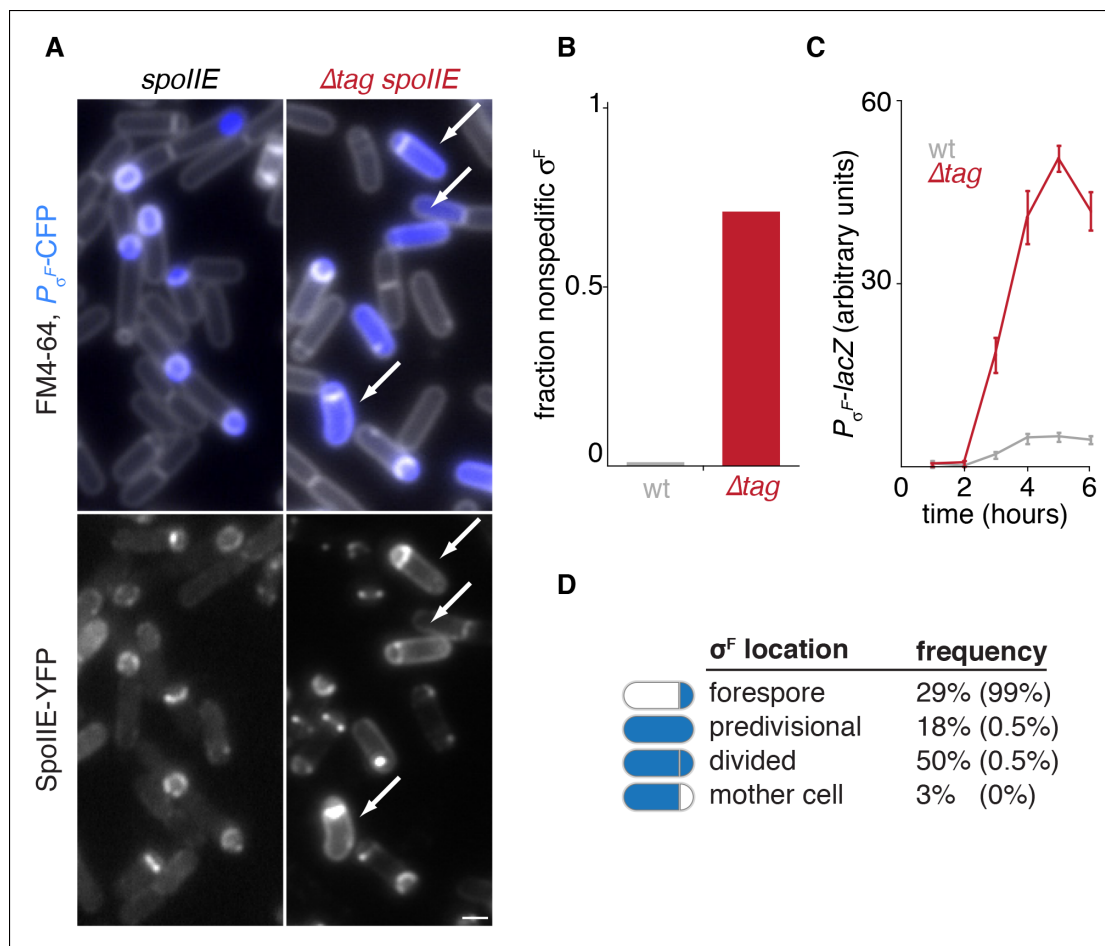


**Figure 3.** Degradation of SpoIIIE is required to compartmentalize SpoIIIE and  $\sigma^F$  activity. (A) Images of sporulating cells producing SpoIIIE-YFP (left, strain RL5876) or  $\Delta$ Tag SpoIIIE-YFP (right, strain RL5892). Top images show CFP (blue) produced under the control of the  $\sigma^F$  dependent *spoIIQ* promoter and FM4-64-stained membrane (white); bottom images show SpoIIIE-YFP. White arrows indicate cells with uncompartimentalized  $\sigma^F$  activity and SpoIIIE in the mother cell. The contrast for images of SpoIIIE-YFP has been adjusted to approximately 5X brighter than for  $\Delta$ Tag-SpoIIIE-YFP for display purposes. Scale bar: 1  $\mu$ m. (B) Quantification of the forespore specificity of  $\sigma^F$  activity from hundreds of cells from images as shown in panel A. (C)  $\sigma^F$  activity was measured during sporulation using a translational fusion of the  $\sigma^F$  dependent *SpolIIQ* promoter to LacZ (wt SpoIIIE strain RL5893,  $\Delta$ Tag SpoIIIE strain RL5894). Time after initiation of sporulation is indicated, and error bars represent the standard deviation from three biological replicates. (D) Quantification of the dependence of  $\sigma^F$  activation on asymmetric cell division driven by  $\Delta$ Tag-SpoIIIE. Hundreds of cells from images as shown in panel A were manually assessed for completion of asymmetric cell division and compartmentalization of  $\sigma^F$  activity. The percent of cells with each pattern of  $\sigma^F$  activity is indicated for  $\Delta tag$ -spoIIIE cells (values for wt spoIIIE cells are indicated in parenthesis).

DOI: 10.7554/eLife.08145.008

The following figure supplements are available for Figure 3:

**Figure supplement 1.** FtsH is active in the forespore.

DOI: 10.7554/eLife.08145.009

To identify features of SpoIIIE required for its accumulation in the forespore, we screened for SpoIIIE variants defective in compartmentalization. We created amino acid substitutions of the most highly conserved residues in SpoIIIE and tested these variants (and previously described variants) for function in sporulation (Figure 4A, Figure 4—source data 1) and forespore accumulation (Figure 4B). To monitor accumulation in the forespore of each SpoIIIE variant, we compiled average profiles of SpoIIIE-YFP along the long axis of hundreds of cells that had undergone polar division. Through this analysis, we identified nine variants of SpoIIIE (for example SpoIIIE<sup>K356D</sup>) that were absent in the forespore (Figure 4A,B blue) and accumulated to reduced levels (Figure 4C). Variants with normal compartmentalization, in contrast, accumulated at approximately wild-type levels (Figure 4B,C black). Supporting the idea that failure to accumulate in the forespore was due to unrestricted, FtsH-dependent degradation, removal of Tag<sup>SpoIIIE</sup> restored these SpoIIIE mutant proteins to

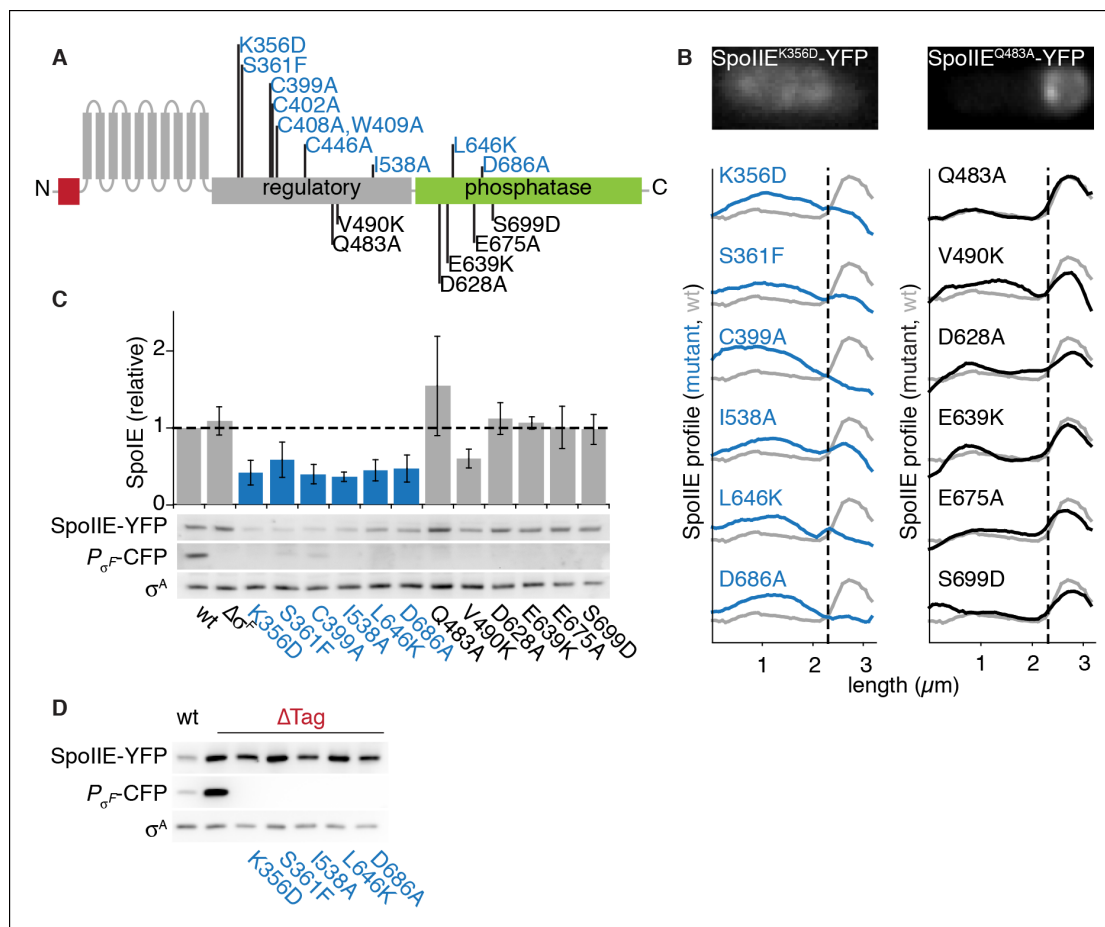


**Figure 4.** SpoIIE stabilization and localization mutants. (A) Diagram of SpoIIE mutants with sporulation defects. Variants with localization and  $\sigma^F$  activation defects are shown above the diagram in blue, and variants with normal localization but defects in  $\sigma^F$  activation are shown below the diagram in black. (B) Localization of SpoIIE mutants. Hundreds of asymmetrically divided cells were aligned at the forespore pole to generate average profiles of SpoIIE-YFP localization for each SpoIIE mutant (strains RL5895–5909) with a reference plot (gray) from wild-type SpoIIE-YFP from  $\sigma^F$  mutant cells (strain RL5910). The dashed line represents the approximate position of the asymmetric septum. Images of representative cells with the mislocalized variant SpoIIE<sup>K356D</sup> (left, strain RL5895) and forespore-localized SpoIIE<sup>Q483A</sup> (right, strain RL5904) are shown. (C) Western blots of protein levels in SpoIIE mutant strains shown in panel B probed for SpoIIE-YFP (with  $\alpha$ -GFP antibody), CFP produced under the control of a  $\sigma^F$ -driven promoter, and  $\sigma^A$  as a loading control. Levels of each SpoIIE variant were normalized to wt SpoIIE (strain RL5876). Error bars represent the standard deviation from three biological replicates. All localization mutants (shown in blue) are different from the  $\sigma^F$  mutant control with p values less than 0.0025 from a paired t-test. (D) Western blots of SpoIIE compartmentalization mutants with Tag<sup>SpoIIE</sup> removed (strains RL5911–5916, with strain RL5876 as a reference) as in panel C.

DOI: 10.7554/eLife.08145.010

The following source data and figure supplements are available for figure 4:

**Source data 1.** Sporulation efficiency of SpoIIE mutants.

DOI: 10.7554/eLife.08145.011

**Figure supplement 1.** An allele specific suppressor of SpoIIE<sup>K356D</sup> rescues compartmentalization and stabilization.

DOI: 10.7554/eLife.08145.012

levels several-fold higher than for wild-type SpoIIE and equivalent to  $\Delta$ Tag SpoIIE (Figure 4D). We conclude that SpoIIE undergoes a transition in the forespore that protects it from FtsH-dependent proteolysis and that this transition is blocked by amino acid substitutions such as K356D.

Additionally, we tested whether stabilization of the SpoIIE mutant proteins was sufficient to support  $\sigma^F$  activation independent of their susceptibility to degradation. We found that even when Tag<sup>SpoIIE</sup> was removed, the mutant proteins failed to activate  $\sigma^F$  (Figure 4D middle panel). A simple unifying model is that the proposed, K356-dependent conformational rearrangement that protects SpoIIE from proteolysis in the forespore is also required to allow it to activate  $\sigma^F$ .



## An allele-specific suppressor of SpoII<sup>E</sup><sup>K356D</sup>

To investigate the link between stabilization, compartmentalization and activation of SpoII<sup>E</sup>, we selected for and isolated several suppressors that restored sporulation to the compartmentalization-defective mutant SpoII<sup>E</sup><sup>K356D</sup>. We chose this mutant because the K356D substitution was located in the regulatory domain of SpoII<sup>E</sup> and caused a particularly severe sporulation defect. We isolated intragenic suppressors at two codons in an apparently saturating screen (see Materials and methods, **Figure 4—source data 1** and **Figure 4—figure supplement 1**). One of them, causing a T353I substitution, was allele-specific (it suppressed SpoII<sup>E</sup><sup>K356D</sup> but not SpoII<sup>E</sup><sup>S361F</sup> or SpoII<sup>E</sup><sup>V490K</sup>, **Figure 4—source data 1**). The T353I substitution restored SpoII<sup>E</sup><sup>K356D</sup> to wild-type protein levels (**Figure 4—figure supplement 1B**), partially restored restriction of SpoII<sup>E</sup><sup>K356D</sup> to the forespore (**Figure 4—figure supplement 1C**), and restored compartment-specific  $\sigma^F$  activation (**Figure 4—figure supplement 1D**). The coordinated rescue of these phenotypes by a single amino acid substitution supports our model that a common feature of SpoII<sup>E</sup> mediates protection from proteolysis, accumulation in the forespore, and activation of  $\sigma^F$ .

The other intragenic suppressors of SpoII<sup>E</sup><sup>K356D</sup> were substitutions at V697 (V697A and V697F), which is located in the phosphatase domain of SpoII<sup>E</sup>. V697A had been independently isolated previously and shown to cause premature activation of  $\sigma^F$  (in the absence of the K356D substitution) (**Hilbert and Piggot, 2003**). These suppressors were not allele specific; V697A suppressed all other mutants of SpoII<sup>E</sup>, including the compartmentalization defective SpoII<sup>E</sup><sup>S361F</sup> mutant and the compartmentalized SpoII<sup>E</sup><sup>Q483A</sup> mutant (**Figure 4—source data 1**, [Carniol et al., 2004]). The V697A substitution did not restore compartmentalization or stabilization of SpoII<sup>E</sup>. It did restore  $\sigma^F$  activation but not compartmentalization of  $\sigma^F$  activity (**Figure 4—source data 1** and **Figure 4—figure supplement 1**). All together, these results suggest that the V697A substitution locks the phosphatase domain in a high activity state, bypassing the activation defect of SpoII<sup>E</sup><sup>K356D</sup>. Indeed, biochemical experiments showed that the V697A substitution enhanced the activity of SpoII<sup>E</sup> in dephosphorylating SpoIIAA-P (**Figure 4—figure supplement 1E**).

## SpoII<sup>E</sup> is compartmentalized and stabilized by binding to the cell pole

To further investigate the mechanism of SpoII<sup>E</sup> compartmentalization, we took advantage of the compartmentalization-defective variant SpoII<sup>E</sup><sup>K353D</sup> and revisited the localization of stabilized SpoII<sup>E</sup>. To isolate events prior to  $\sigma^F$  activation, and because certain targets of  $\sigma^F$  (e.g. SpoIIQ) affect the localization of SpoII<sup>E</sup> (**Campo et al., 2008**), we used a mutant lacking  $\sigma^F$  to analyze the localization of SpoII<sup>E</sup>,  $\Delta$ Tag-SpoII<sup>E</sup>, and its K353D mutant derivative (in contrast to the experiment of **Figure 3A** in which cells were  $\sigma^F$ ).

Our most striking observation was that  $\Delta$ Tag-SpoII<sup>E</sup> was noticeably enriched at the poles of cells that had not initiated polar division (**Figure 5A**). Polar enrichment was dependent on stabilization by removal of Tag<sup>SpoII<sup>E</sup></sup> (**Figure 5A** gray line). Because the forespore is derived from the cell pole, we hypothesized that the pole is a landmark that directs SpoII<sup>E</sup> compartmentalization. In support of this idea, polar localization was abolished by the K356D substitution and partially restored by the T353I suppressor (**Figure 5A** lower panel). Thus, the pole is a cue that directs compartmentalization of SpoII<sup>E</sup>, and the same feature(s) of SpoII<sup>E</sup> that is required for polar recognition is also required for stabilization and  $\sigma^F$  activation.

We next asked whether SpoII<sup>E</sup> has an intrinsic affinity for the cell pole or whether SpoII<sup>E</sup> is captured there by features unique to cells undergoing sporulation. To address this question, we engineered the synthesis of SpoII<sup>E</sup>-YFP and  $\Delta$ Tag SpoII<sup>E</sup>-YFP in vegetative cells that were blocked in divisome formation through the use of the FtsZ inhibitor MciZ (**Handler et al., 2008**). We observed that  $\Delta$ Tag SpoII<sup>E</sup>-YFP was enriched at the ends of these cells, and this localization recapitulated the features of polar localization seen during sporulation: polar localization was only observed for stabilized SpoII<sup>E</sup>, was blocked by K356D substitution, and was restored by the T353I suppressor (**Figure 5B**). Therefore, a fundamental, constitutive feature of the cell pole mediates SpoII<sup>E</sup> polar localization.

We next sought to identify the feature of the pole that is responsible for SpoII<sup>E</sup> localization. DivIVA recognizes the negative curvature of the cell pole and directs the polar localization of several other proteins during growth and sporulation (**Lenarcic et al., 2009; Ramamurthi and Losick, 2009**). Recently, DivIVA was shown to co-immunoprecipitate with SpoII<sup>E</sup>, making it an attractive

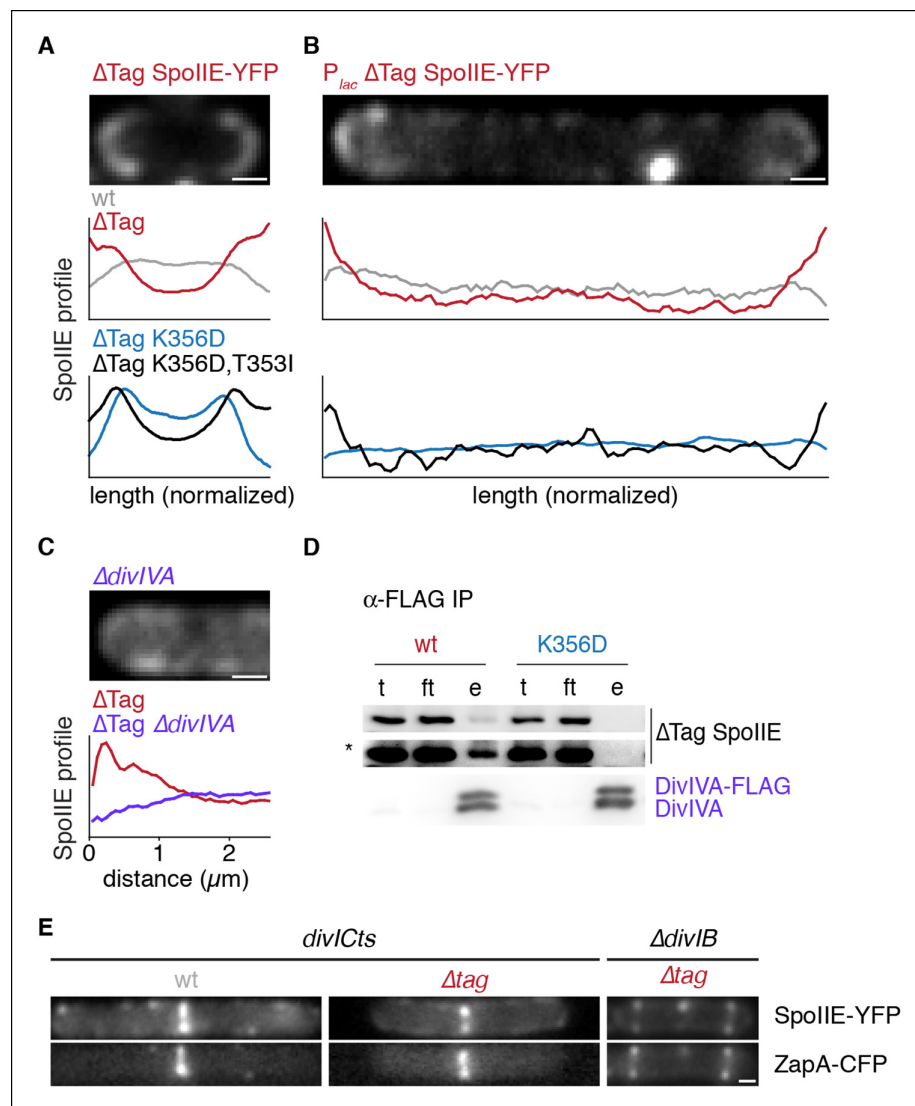


**Figure 5.** Stabilized SpoIIIE localizes to the cell pole. (A) Average profiles of SpoIIIE-YFP from undivided sporulating cells lacking  $\sigma^F$  activity are shown (strains RL5910, 5917, 5912, 5918), with a representative cell with  $\Delta$ Tag-SpoIIIE-YFP (strain RL5917) displayed above. (B) Vegetatively growing cells expressing SpoIIIE-YFP (strains RL5919-5922) displayed as in panel A; variants as indicated. (C) MciZ-expressing cells ( $\Delta$ divIVA [strain RL5923] or otherwise wildtype [strain RL5924]) were imaged as in panel B and average profiles of  $\Delta$ Tag-SpoIIIE-YFP were generated from 20 randomly selected cell poles. (D) DivIVA-FLAG was immunoprecipitated with  $\alpha$ -FLAG magnetic beads from extracts of sporulating cells expressing SpoIIIE variants as indicated (strains RL5925, 5926), and detected by Western blot. The elution (e) shown is 100X concentrated relative to the load (l) and flowthrough (ft) samples. Blots were probed with  $\alpha$ -GFP antibody (top two images; lower image in high contrast\*) and  $\alpha$ -DivIVA antisera (below). Because DivIVA oligomerizes, untagged DivIVA is also co-immunoprecipitated. (E) SpoIIIE preferentially localizes to the divisome rather than the pole. Representative cells expressing SpoIIIE-YFP and CFP-ZapA are shown. Left images show exponentially growing *divICts* cells (strains RL5927, 5928), and right images show a sporulating  $\Delta$ divIB cell (strain RL5929). Scale bars indicate 0.5  $\mu$ m in all panels.

DOI: [10.7554/eLife.08145.013](https://doi.org/10.7554/eLife.08145.013)

The following figure supplements are available for Figure 5:

**Figure supplement 1.** Transcription of *spoIIIE* in the forespore is not required to compartmentalize SpoIIIE.

DOI: [10.7554/eLife.08145.014](https://doi.org/10.7554/eLife.08145.014)

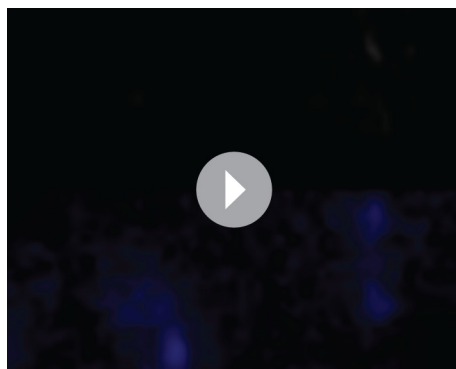
candidate to anchor SpoII<sub>E</sub> to the cell pole (Eswaramoorthy *et al.*, 2014). We found that whereas wild-type SpoII<sub>E</sub> co-immunoprecipitated with DivIVA from extracts of sporulating cells (as previously observed), SpoII<sub>E</sub><sup>K356D</sup> did not (Figure 5D). Additionally ΔTag SpoII<sub>E</sub>-YFP polar localization during vegetative growth was abolished by a *divIVA* deletion (in the background of a *minD* deletion to suppress the cell division defect of *divIVA* deletion) (Figure 5C). Thus, DivIVA directly or indirectly anchors SpoII<sub>E</sub> at the cell pole and can do so independently of sporulation. Based on the result with the K356D mutant, we further propose that this anchoring serves to stabilize, compartmentalize and activate SpoII<sub>E</sub>, and that these activities are linked through a common feature of SpoII<sub>E</sub>.

### The divisome competes with the cell pole for binding of SpoII<sub>E</sub>

During sporulation, SpoII<sub>E</sub> first accumulates at the polar divisome, constricts along with the septum and then is released into the forespore following the completion of cytokinesis (as shown by time-lapse and structured illumination microscopy in Figure 1C, Videos 1–3, Figure 1—figure supplement 1). This suggests that the divisome competes with the pole for SpoII<sub>E</sub> binding and that SpoII<sub>E</sub> is not free to associate with the pole until the divisome is disassembled. To investigate this model, we monitored SpoII<sub>E</sub> localization in the background of a temperature-sensitive allele of *divIC* that stalls cell division after divisome formation but before cytokinesis (Levin and Losick, 1994). In this background, SpoII<sub>E</sub>-YFP and ΔTag SpoII<sub>E</sub>-YFP localized to the divisome (as visualized with a ZapA-CFP fusion) but not to the cell pole (Figure 5E). Similarly, when cytokinesis was blocked during sporulation by a *divB* deletion (Thompson *et al.*, 2006), ΔTag SpoII<sub>E</sub>-YFP localized to the divisome but not to the cell pole (Figure 5E). Therefore, the divisome sequesters and prevents SpoII<sub>E</sub> from associating with the cell pole. We conclude that SpoII<sub>E</sub> has affinity for two subcellular sites: the divisome, its dominant binding site, and the pole, where it is captured only after release from the divisome after the completion of cytokinesis.

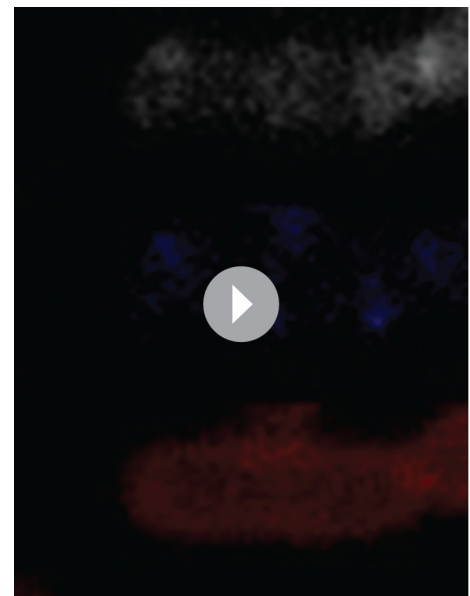
### SpoII<sub>E</sub> is compartmentalized in vegetative cells engineered to divide asymmetrically

The results discussed above suggest a simple model for how SpoII<sub>E</sub> and  $\sigma^F$  activity are compartmentalized in the forespore. We propose that SpoII<sub>E</sub> is sequestered at the asymmetrically positioned divisome and is released and captured at the proximal (forespore) pole when cytokinesis is completed. In support of this idea, cells that cannot synthesize additional SpoII<sub>E</sub> molecules in the forespore nonetheless robustly compartmentalize SpoII<sub>E</sub> (Figure 5—figure supplement 1). Asymmetric compartmentalization of SpoII<sub>E</sub> in the forespore could be achieved by virtue of the



**Video 2.** Movie file of the sporulating cell shown in Figure 1—figure supplement 1A (2fps). SpoII<sub>E</sub>-YFP is shown in grey, and the divisome marked by CFP-ZapA is shown in blue.

DOI: 10.7554/eLife.08145.015



**Video 3.** Movie file of the sporulating cell shown in Figure 1—figure supplement 1B (2fps). SpoII<sub>E</sub>-YFP is shown in grey, the divisome marked by CFP-ZapA is shown in blue, and the membrane marked by MalFtm-mNeptune is shown in red.

DOI: 10.7554/eLife.08145.016

close proximity of the divisome and the forespore pole. Weak SpoIIIE association with the pole would be compensated for by the small volume of the forespore and reinforced by protection from degradation by FtsH. Finally, any SpoIIIE released into the mother cell would be captured at the divisome, preventing capture at the mother cell pole. Thus, a simple model explains how SpoIIIE is protected from degradation and compartmentalized in the forespore only after cytokinesis is complete.

The heart of this model is that asymmetric positioning of the division septum is all that is necessary for compartment specific stabilization and activation of SpoIIIE. To test this prediction, we sought to compartmentalize SpoIIIE in cells that had been engineered to undergo polar division independently of sporulation. To do so, we artificially expressed *spoIIIE* and overexpressed *ftsAZ* in vegetative cells, which was previously demonstrated to reposition the division septum from the mid-cell to near the pole (Ben-Yehuda and Losick, 2002). To preclude transcription of sporulation-specific genes, we additionally deleted the master regulator for entry into sporulation, *spo0A*. We then visualized the localization of SpoIIIE in these cells. As predicted by our model, cells enriched for SpoIIIE were much smaller than average for the entire population (Figure 6A,B). Further, to ask whether this compartmentalization of SpoIIIE was sufficient to direct cell-specific activation of  $\sigma^F$ , we additionally induced synthesis of  $\sigma^F$  and its regulators SpoIIAA (the anti-anti  $\sigma^F$  factor substrate for the SpoIIIE phosphatase) and SpoIIAB (the anti- $\sigma^F$  factor) in a strain harboring a reporter for  $\sigma^F$  activity. Remarkably,  $\sigma^F$  was activated with high selectivity in a subpopulation of the minicells (Figure 6A,B). We conclude that polar division is the only feature of sporulation necessary to restrict SpoIIIE protein and activity to the small cell and that this is sufficient to explain compartmentalized activation of  $\sigma^F$ .

### Multimerization of SpoIIIE is required for polar anchoring and activation of $\sigma^F$

To gain insight into the molecular mechanism of SpoIIIE localization and activation, we expressed and purified the C-terminal cytosolic domain of SpoIIIE (residues 320 to 827, SpoIIIE<sup>320-827</sup>) for biochemical characterization. A striking feature of SpoIIIE<sup>320-827</sup> was that it multimerizes, and analytical ultracentrifugation revealed these multimers to be hexamers and higher order assemblies of hexamers (Figure 7A).

To identify determinants of multimerization and its role for SpoIIIE function, we made serial N-terminal truncations of SpoIIIE starting at residue 320 and determined the oligomeric state of

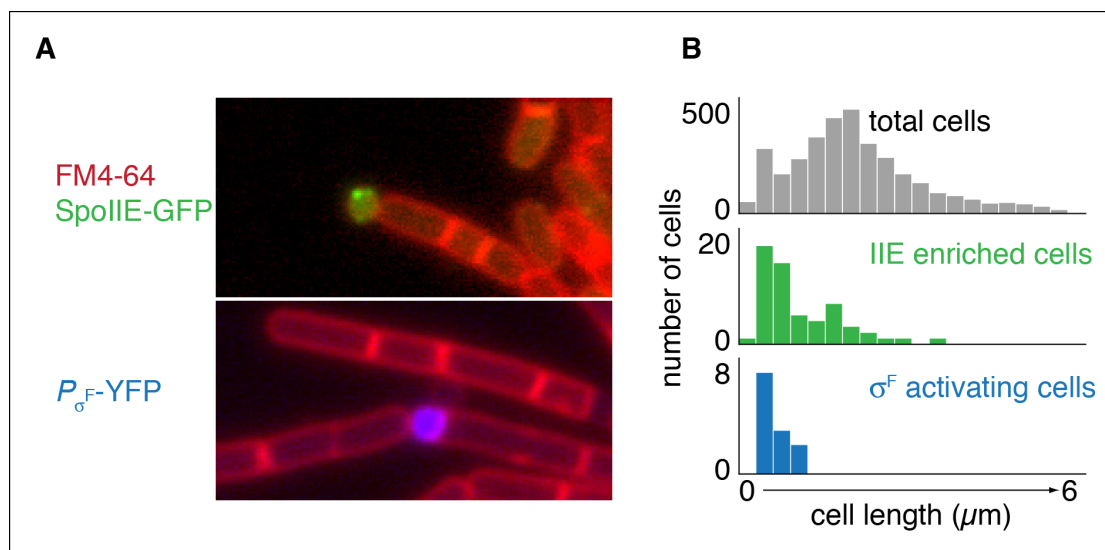


**Figure 6.** Repositioning the septum in vegetative cells is sufficient for compartmentalization of SpoIIIE. (A) In the top image, vegetatively growing cells producing SpoIIIE-GFP and overexpressing the *ftsZ* operon formed minicells enriched for SpoIIIE-GFP (strain RL5930). In the lower image, cells additionally expressed the *spoIIA* operon and harbored a YFP reporter for  $\sigma^F$  activity (strain RL5931). (B) Quantification of images as shown in panel A. SpoIIIE enriched cells (representing 56 out of 3168 total cells) are shown in green in the middle plot and are defined as cells with 2 standard deviations above the mean SpoIIIE-GFP intensity. Cells that had active  $\sigma^F$  were rare in the population (12 cells) and were identified based on detectable levels of YFP fluorescence and their sizes were measured. They are shown in blue at the bottom.

DOI: 10.7554/eLife.08145.017

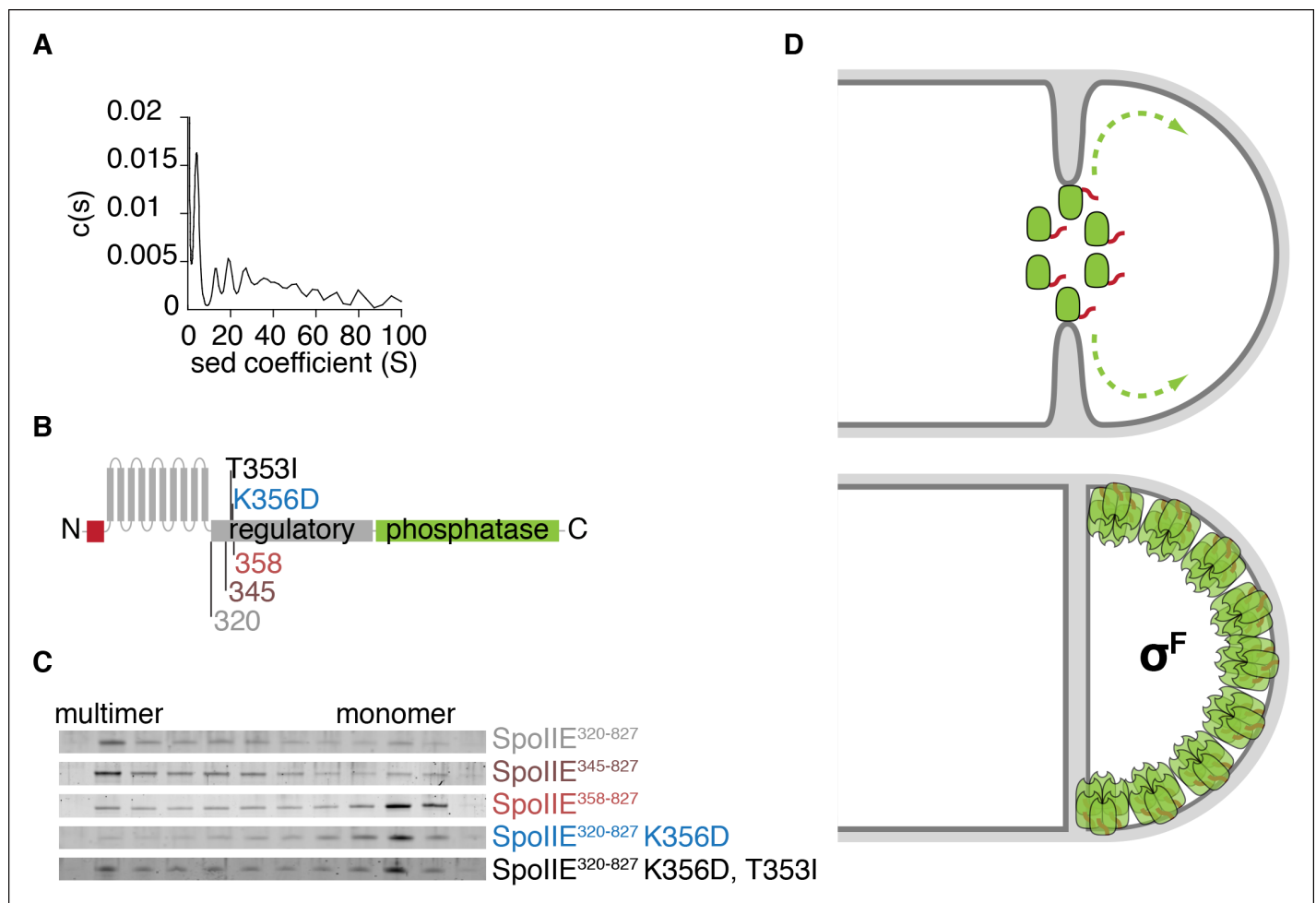


**Figure 7.** Multimerization is required for compartmentalization of SpoIIIE and  $\sigma^F$  activation. (A) Purified soluble SpoIIIE<sup>320-827</sup> was analyzed by sedimentation velocity analytical ultracentrifugation detected by absorbance at 280nm and fitted to  $c(s)$  using Sedfit. Peaks corresponding to the predicted sedimentation coefficient for monomeric SpoIIIE, hexamers, and multimers of hexamers were observed. (B) Diagram of the mutations and truncations in SpoIIIE analyzed in panel C. (C) Multimerization of SpoIIIE variants was analyzed by gel filtration with a 24 ml Superose 6 column. 1 ml fractions from 7–18 ml of the run were collected, run on SDS-PAGE gels, and stained with SYPRO Ruby. (D) Model for handoff of SpoIIIE from the divisome to the adjacent cell pole. SpoIIIE (green) initially accumulates at the divisome and constricts along with FtsZ during cytokinesis. Prior to the completion of cell division, SpoIIIE is degraded by FtsH through its Tag<sup>SpoIIIE</sup> (red). (We cannot distinguish whether association with the divisome protects SpoIIIE from proteolysis or if SpoIIIE turns over while associated with the divisome.) Upon the completion of cytokinesis, SpoIIIE transfers to the adjacent cell pole where multimerization protects it from proteolysis (as depicted by the light orange Tags) and leads to phosphatase activation. We propose that close proximity favors transfer to the immediately adjacent pole and that concentration of SpoIIIE in the forespore, which is almost entirely derived from the pole, promotes multimerization.

DOI: [10.7554/eLife.08145.018](https://doi.org/10.7554/eLife.08145.018)

The following figure supplements are available for Figure 7:

**Figure supplement 1.** SpoIIIE variants defective for sporulation multimerize.

DOI: [10.7554/eLife.08145.019](https://doi.org/10.7554/eLife.08145.019)

each by gel filtration (Figure 7B,C). We found that the 13-amino acid interval from residues 345 to 358 contained a feature required for multimerization; although SpoIIIE truncated to residue 345 (SpoIIIE<sup>345-827</sup>) multimerized, all truncations extending to 358 (SpoIIIE<sup>358-827</sup>) and beyond did not (Figure 7C). This region encompasses K356, raising the possibility that K356D might block stabilization and activation of SpoIIIE at the pole by blocking multimerization, and that T353I might suppress the phenotypes of K356D by restoring multimerization. Indeed, gel filtration experiments confirmed that SpoIIIE<sup>320-827</sup>, K356D did not multimerize and that T353I partially restored multimerization (Figure 7C). Of all the SpoIIIE variants analyzed, the K356D substitution uniquely blocked

multimerization, highlighting a key role for the N-terminal region of the regulatory domain in mediating multimerization (**Figure 7—figure supplement 1**).

In sum, these biochemical experiments in conjunction with the *in vivo* experiments described above lead us to propose that multimerization of SpoII $\epsilon$  is the critical transition that stabilizes SpoII $\epsilon$ , enabling it to recognize the cell pole and leading to its activation as a phosphatase. First, we found that multimerization is required for stabilization of SpoII $\epsilon$  and compartmentalization of SpoII $\epsilon$  to the forespore (**Figure 4B,C—figure supplement 1**). Second, removal of Tag<sup>SpoII $\epsilon$</sup>  uncoupled multimerization from degradation, and revealed an additional link between SpoII $\epsilon$  activation and multimerization (**Figure 4D**). Finally, we found that recognition of the cell pole by SpoII $\epsilon$  also depended on multimerization, even when SpoII $\epsilon$  was synthesized in vegetative cells uncoupled from degradation and  $\sigma^F$  activation (**Figure 5B**).

## Discussion

A hallmark of sporulation is a process of asymmetric division that creates a septum near one randomly selected pole of the cell. Polar placement of the septum directs the protein phosphatase SpoII $\epsilon$  to activate  $\sigma^F$  in the resulting forespore. How SpoII $\epsilon$  activates  $\sigma^F$  at the right time and in the right place has been one of the enduring mysteries of this developmental system. As the end of the cell used for asymmetric division is chosen without regard to whether it is the old or new pole (**Veening et al., 2008**), the cues that SpoII $\epsilon$  interprets to achieve cell-specific activation of  $\sigma^F$  must arise *de novo*, that is, from the position of the septum rather than from preexisting asymmetry. Indeed, our results show that no feature of the sporulation process other than polar placement of the septum is necessary for compartmentalizing SpoII $\epsilon$  and for cell-specific activation of  $\sigma^F$  (**Figure 6**). In addition, as transcription of *spoII $\epsilon$*  commences prior to asymmetric division (**Fujita and Losick, 2003**) (**Figure 2A**), SpoII $\epsilon$  must also respond to temporal cues to ensure it is not active prior to the completion of cytokinesis.

Here we have provided evidence for a model in which SpoII $\epsilon$  leverages the asymmetric position of the septum to selectively associate with the adjacent cell pole of the forespore where it is stabilized and activated (**Figure 7D**). Three key features of our model are as follows:

1. *Capture at the cell pole.* SpoII $\epsilon$  initially accumulates at the polar divisome and is handed off to the forespore pole following cytokinesis. Sequential transfer is enforced by preferential binding to the divisome over the cell pole, and we propose that selectivity for the forespore is achieved by the divisome being immediately adjacent to the forespore pole and that the forespore is largely derived from the pole. Additionally, SpoII $\epsilon$  not captured in the forespore would be sequestered at the distal divisome in the newly formed mother cell, preserving asymmetry.
2. *Spatially restricted proteolysis.* SpoII $\epsilon$  is degraded by the AAA+ protease FtsH and is selectively stabilized in the forespore. This ensures that SpoII $\epsilon$  does not accumulate or become active prior to asymmetric division or in the mother cell following asymmetric division.
3. *Oligomerization.* Polar recognition, protection from FtsH, and activation as a phosphatase are linked by a transition that takes place at the pole and is mediated by oligomerization.

Together these three features provide a simple mechanism for how cues derived from asymmetric cell division restrict SpoII $\epsilon$  to the forespore and couple  $\sigma^F$  activation to the completion of cytokinesis. At the same time our model raises several unanswered questions important both for understanding sporulation and diverse related biological systems.

How does SpoII $\epsilon$  localize to the cell pole and the divisome? Localization to the divisome depends on FtsZ and FtsA, the earliest assembling proteins to define the divisome (**Levin et al., 1997**). But whether SpoII $\epsilon$  interacts with these proteins directly, what features of SpoII $\epsilon$  mediate divisome association, and how SpoII $\epsilon$  influences FtsZ polymerization and divisome maturation are unknown. Answering these questions will help us to understand how SpoII $\epsilon$  is transferred from the divisome to the cell pole as well as how SpoII $\epsilon$  influences the position of the division septum. Similarly, localization to the pole depends on DivIVA, which directly senses the shape of the pole and acts as an organizing center for other pole-associated proteins (**Lenarcic et al., 2009; Ramamurthi and Losick, 2009**). But it is not known whether this interaction is direct or depends on an accessory protein.

How does oligomerization of SpoII $\epsilon$  promote  $\sigma^F$  activation? Genetic and biochemical evidence are consistent with a model in which stabilization, compartmentalization, and activation of SpoII $\epsilon$  are



linked by oligomerization of SpoII $\epsilon$  molecules and that this oligomerization takes place in the forespore after asymmetric division. We cannot exclude the possibility, however, that oligomerization commences earlier in sporulation and that some other unrecognized feature of SpoII $\epsilon$  is additionally required for its transition to a stable and active state in the forespore. Structural information about the organization of SpoII $\epsilon$  oligomers and an *in vivo* assay for oligomerization may help distinguish between these possibilities and yield new insights into how it contributes to compartment specific  $\sigma^F$  activation.

How is activation of  $\sigma^F$  coordinated with the completion of asymmetric cell division? Our model proposes two mechanisms to prevent predivisional activation of  $\sigma^F$ : First, the features of the forespore (small size, high concentration of cell pole, and proximity to the divisome) that promote SpoII $\epsilon$  stabilization and  $\sigma^F$  activation are all emergent properties that depend on completion of cell division. Second, competition between the divisome and cell pole for binding to SpoII $\epsilon$  prevents premature accumulation and activation of  $\sigma^F$ . Although there has been uncertainty about when SpoII $\epsilon$  is released from the divisome and when asymmetry in SpoII $\epsilon$  compartmentalization is established (Eswaramoorthy *et al.*, 2014; Lucet *et al.*, 2000; Wu *et al.*, 1998), our time-lapse imaging and structured illumination microscopy indicate that SpoII $\epsilon$  constricts along with the FtsZ ring during cytokinesis (Figure 1, Figure 1—figure supplement 1). This is consistent with our model that SpoII $\epsilon$  remains sequestered at the divisome until cytokinesis is completed. In the future it will be important to determine just how association with the divisome prevents SpoII $\epsilon$  from oligomerizing and activating  $\sigma^F$ .

How is SpoII $\epsilon$  protected from degradation in the forespore? We have shown that the N-terminal tail of SpoII $\epsilon$  is necessary and sufficient for FtsH-dependent degradation (Figure 2E,F) and that stabilization in the forespore is mediated by features of SpoII $\epsilon$  that are required for interaction with the cell pole (Figure 3,4). Additionally, we have presented evidence that multimerization of SpoII $\epsilon$  is required for both stabilization and interaction with the pole. One possibility is that multimerization shields the Tag<sup>SpoII $\epsilon$</sup>  from FtsH as depicted in Figure 7D. Alternatively, as FtsH has been shown to have weak unfoldase activity (Herman *et al.*, 2003), multimerization might render SpoII $\epsilon$  resistant to FtsH unfolding and hence proteolysis. Finally, although we favor the view that SpoII $\epsilon$  is directly recognized by FtsH, it is conceivable that it requires an adaptor as is the case for some substrates of AAA+ proteases (Gottesman, 2003). If so, SpoII $\epsilon$  could be protected from degradation by negative regulation of the adaptor.

How is the phosphatase activity of SpoII $\epsilon$  regulated? Our genetic analysis provides clues for how activation occurs. We found that the V697A substitution locks SpoII $\epsilon$  in a high activity state *in vitro*, and restores  $\sigma^F$  activity in mutants defective for compartmentalization and  $\sigma^F$  activation. V697 is in an active site proximal loop (Levdikov *et al.*, 2011); in many PP2C phosphatases this loop coordinates a third manganese ion that is critical for activity (Su *et al.*, 2011). However, SpoII $\epsilon$  lacks the aspartate that coordinates this manganese, which could indicate that V697A locks the phosphatase in a conformation that compensates for the missing manganese ion. Additionally, we found that the stimulation of phosphatase activity (and binding to the pole) is genetically linked to multimerization: oligomerization, and  $\sigma^F$  activation were blocked by the substitution K356D and restored by T353I. We therefore speculate that multimerization induces a conformational change that organizes the catalytic center, compensating for the missing manganese and activating the phosphatase. A test of our hypothesis for a multimerization-dependent conformational change in the active site will require reconstituting multimerization-dependent activation of SpoII $\epsilon$  *in vitro*. Other PP2C phosphatases, such as the tumor suppressor protein PHLPP (Gao *et al.*, 2005), similarly lack the aspartate to coordinate a third magnesium ion, suggesting that our speculation, if correct, could represent a more general regulatory mechanism for PP2C phosphatases.

In summary, we propose that the asymmetrically positioned division machinery – the *de novo* generated source of asymmetry – positions SpoII $\epsilon$  to be captured at the adjacent cell pole, triggering  $\sigma^F$ -directed gene expression in the forespore. Capture at the pole, proteolytic stabilization and stimulation of the phosphatase all depend on oligomerization of SpoII $\epsilon$ . Thus, three interlinked regulatory events are sufficient to explain how SpoII $\epsilon$  exploits a stochastically generated spatial cue to the cell-specific activation of a transcription factor.

## Materials and methods

### Strains and strain construction

*B. subtilis* strains were constructed in PY79 using standard molecular genetic techniques (Harwood and Cutting, 1990). Full details of strain genotypes, and construction are provided in **Supplementary file 1**. For IPTG dependent expression ( $P_{lac}$ ), the hyperspank promoter was used (from pDR111a, gift of David Rudner), and for  $\sigma^F$  dependent expression ( $P_{\sigma F}$ ), the *spoIIQ* promoter was used. Constructs were made by Gibson Assembly (New England Biolabs, Ipswich, MA), and point mutations were introduced using QuikChange mutagenesis (Agilent Technologies).

### Isolation of suppressors

Suppressors of the *spoII*E-K356D mutation were isolated by growing 100 ml cultures of strain RL5895 in DSM sporulation medium at 37°C for 28 hr. 11 ml of cells were heat killed at 80°C and used to re-inoculate a new 100 ml DSM culture. Heat killed cells from the second round culture were plated on DSM agar plates. Genomic DNA was prepared from the strain and retransformed to strain RL5875, lacking *spoII*E, to confirm linkage to *spoII*E, and the *spoII*E locus was sequenced. Finally, suppressor mutations were then reconstructed by quickchange mutagenesis. Mutations T353I, V697A, V697F, and pseudorevertants K356T and K356Y were each isolated from multiple independent cultures, suggesting that the screen was near saturation.

### Protein degradation and protein levels

Protein degradation rates were measured by shutting off translation by addition of chloramphenicol (100 µg/ml) to cultures. Samples were removed at indicated timepoints and immediately put on ice. Cells were lysed by mechanical disruption in a FastPrep (MP-BIO, Santa Ana, CA). Western blots were conducted by standard procedures and imaged on a BioRad ChemiDoc imager using chemiluminescence. Antibodies used were polyclonal anti-GFP (Rudner and Losick, 2002), polyclonal anti- $\sigma^A$  (Fujita, 2000), polyclonal anti-DivIVA (Eswaramoorthy et al., 2014), and monoclonal anti-FLAG M2 (Sigma Aldrich, St. Louis, MO). Standards were used to determine linearity in each experiment. Immunoprecipitation of DivIVA was performed as published (Eswaramoorthy et al., 2014).

### Fluorescence microscopy

All micrographs were acquired on an Olympus BX61 upright fluorescence microscope with a 100X objective, with the exception of timelapse images taken on a Nikon ti inverted microscope. Cells were immobilized on 2.5% agarose pads made with sporulation resuspension medium. To quantitatively analyze micrographs, cells were segmented from phase images using either MicrobeTracker (Sliusarenko et al., 2011) or SupperSeggerOpti (Kuwada et al., 2015), and analyzed with custom MatLab scripts (scripts for quantitative image analysis are included as a **Source code 1**). Cell specificity of  $\sigma^F$  activity was determined by analyzing the distribution of  $P_{\sigma F}$ -CFP along the long axis of cells. SpoIIIE localization profiles were calculated for each cell as the normalized ratio of SpoIIIE-YFP to FM4-64 along the long axis of the cell. Because SpoIIIE is a transmembrane protein, FM4-64 accounts for differences in membrane area along the cell axis. For sporulating cells that had undergone division, division septa were detected using FM4-64 and cells were oriented based on the position of the polar septum. Vegetative cells (strains RL5930 and RL5931) were induced to produce minicells by dilution from a log phase overnight culture to OD 0.05 and addition of 1mM IPTG, and 0.25% xylose as appropriate. Cells were imaged after 4 hr of growth at 37°C. Segmentation was performed based on phase images subtracted for FM4-64 to identify division septa in chained cells. Cells enriched for SpoIIIE-GFP were defined as cells with average SpoIIIE-GFP intensity greater than two standard deviations above the mean. Structured illumination microscopy was performed on a Zeiss Elyra microscope in the Harvard Center for Biological Imaging.

### Biochemistry

SpoIIIE was expressed as an N-terminal Sumo-6His fusion in BL21(DE3) cells following overnight induction with 0.5 mM IPTG at 14°C. Cells were lysed in 50 mM Tris pH 8.5, 200 mM NaCl, 1mM beta-mercaptoethanol and purified using HisTrap columns (GE Healthcare, Pittsburg, PA) eluting with a gradient of imidazole. The Sumo-6His tag was removed by cleavage with Ulp1 (Sumo

Protease) followed by Ni-NTA subtraction. For velocity analytical ultracentrifugation, SpoIIIE was dialyzed to 20 mM Tris pH8.5, 100 mM NaCl, 2 mM DTT overnight and data was collected at 280 nM spinning at 20,000 RPM at The Biophysical Instrumentation Facility (NSF-0070319) at MIT. Data were fit to a continuous model using SedFit ([Schuck, 2000](#)). Gel filtration was conducted on a 24 ml Superose 6 column (GE Healthcare, Pittsburg, PA), loading 100  $\mu$ l of 1  $\mu$ M SpoIIIE. Phosphatase assays of soluble fragments of SpoIIIE lacking the transmembrane domain (SpoIIIE<sup>320-827</sup> and SpoIIIE<sup>320-827, V697A</sup>) were performed using <sup>32</sup>P phosphorylated SpoIIAA (phosphorylated by purified SpoIIAB) as a substrate. Multiple turnover reactions were performed with 0.05  $\mu$ M SpoIIIE and varying concentrations of SpoIIAA-P as indicated. Dephosphorylation of SpoIIAA was detected by TLC chromatography on PEI-Cellulose plates developed in 1 M LiCl, 0.8 M Acetic acid.

## Acknowledgements

We dedicate this article to the memory of Patrick J Piggot. We thank T Wilkinson, and I Barak for collaboration and discussions throughout this work, K Ramamurthi and P Eswaramoorthy for discussions and reagents, L Shapiro and J Kardon for valuable comments during manuscript preparation, P Wiggins for code and assistance using SuperSeggerOpti, and A Leech and D Pheasant for assistance with analytical ultracentrifugation.

## Additional information

### Competing interests

RL: Senior Editor, eLife. The other author declares that no competing interests exist.

### Funding

Funder	Grant reference number	Author
National Institutes of Health	GM18568	Richard Losick
Damon Runyon Cancer Research Foundation	DRG 2051-10	Niels Bradshaw

The funders had no role in study design, data collection and interpretation, or the decision to submit the work for publication.

### Author contributions

NB, Conception and design, Acquisition of data, Analysis and interpretation of data, Drafting or revising the article; RL, Conception and design, Analysis and interpretation of data, Drafting or revising the article

## Additional files

### Supplementary files

- Supplementary file 1. Table of strains.

DOI: [10.7554/eLife.08145.020](https://doi.org/10.7554/eLife.08145.020)

- Source code 1. Matlab scripts.

DOI: [10.7554/eLife.08145.021](https://doi.org/10.7554/eLife.08145.021)

## References

- Akiyama Y. 2009. Quality control of cytoplasmic membrane proteins in escherichia coli. *Journal of Biochemistry* **146**:449–454. doi: [10.1093/jb/mvp071](https://doi.org/10.1093/jb/mvp071)
- Anne Levin P, Losick R, Stragier P, Arigoni F. 1997. Localization of the sporulation protein SpoIIIE in *bacillus subtilis* is dependent upon the cell division protein FtsZ. *Molecular Microbiology* **25**:839–846. doi: [10.1111/j.1365-2958.1997.mmi505.x](https://doi.org/10.1111/j.1365-2958.1997.mmi505.x)
- Arigoni F, Guérout-Fleury AM, Barák I, Stragier P. 1999. The SpoIIIE phosphatase, the sporulation septum and the establishment of forespore-specific transcription in *bacillus subtilis*: a reassessment. *Molecular Microbiology* **31**:1407–1415. doi: [10.1046/j.1365-2958.1999.01282.x](https://doi.org/10.1046/j.1365-2958.1999.01282.x)

- Arigoni F, Pogliano K, Webb CD, Stragier P, Losick R. 1995. Localization of protein implicated in establishment of cell type to sites of asymmetric division. *Science* **270**:637–640. doi: [10.1126/science.270.5236.637](https://doi.org/10.1126/science.270.5236.637)
- Barák I, Wilkinson AJ. 2005. Where asymmetry in gene expression originates. *Molecular Microbiology* **57**:611–620. doi: [10.1111/j.1365-2958.2005.04687.x](https://doi.org/10.1111/j.1365-2958.2005.04687.x)
- Ben-Yehuda S, Losick R. 2002. Asymmetric cell division in *b. subtilis* involves a spiral-like intermediate of the cytokinetic protein FtsZ. *Cell* **109**:257–266. doi: [10.1016/S0092-8674\(02\)00698-0](https://doi.org/10.1016/S0092-8674(02)00698-0)
- Bork P, Brown NP, Hegyi H, Schultz J. 1996. The protein phosphatase 2C (p2C) superfamily: detection of bacterial homologues. *Protein Science* **5**:1421–1425. doi: [10.1002/pro.5560050720](https://doi.org/10.1002/pro.5560050720)
- Bowman GR, Lyuksyutova AI, Shapiro L. 2011. Bacterial polarity. *Current Opinion in Cell Biology* **23**:71–77. doi: [10.1016/j.ceb.2010.10.013](https://doi.org/10.1016/j.ceb.2010.10.013)
- Campo N, Marquis KA, Rudner DZ. 2008. SpoIIQ anchors membrane proteins on both sides of the sporulation septum in *Bacillus subtilis*. *The Journal of Biological Chemistry* **283**:4975–4982. doi: [10.1074/jbc.M708024200](https://doi.org/10.1074/jbc.M708024200)
- Carniol K, Eichenberger P, Losick R. 2004. A threshold mechanism governing activation of the developmental regulatory protein sigma f in *Bacillus subtilis*. *The Journal of Biological Chemistry* **279**:14860–14870. doi: [10.1074/jbc.M314274200](https://doi.org/10.1074/jbc.M314274200)
- Diederich B, Wilkinson JF, Magnin T, Najafi M, Errington J, Yudkin MD. 1994. Role of interactions between SpoIIAA and SpoIIAB in regulating cell-specific transcription factor sigma f of *Bacillus subtilis*. *Genes & Development* **8**:2653–2663. doi: [10.1101/gad.8.21.2653](https://doi.org/10.1101/gad.8.21.2653)
- Duncan L, Alper S, Arigoni F, Losick R, Stragier P. 1995. Activation of cell-specific transcription by a serine phosphatase at the site of asymmetric division. *Science* **270**:641–644. doi: [10.1126/science.270.5236.641](https://doi.org/10.1126/science.270.5236.641)
- Duncan L, Losick R. 1993. SpoIIAB is an anti-sigma factor that binds to and inhibits transcription by regulatory protein sigma f from *Bacillus subtilis*. *Proceedings of the National Academy of Sciences of the United States of America* **90**:2325–2329. doi: [10.1073/pnas.90.6.2325](https://doi.org/10.1073/pnas.90.6.2325)
- Eswaramoorthy P, Winter PW, Wawrzusin P, York AG, Shroff H, Ramamurthi KS, Søgaard-Andersen L. 2014. Asymmetric division and differential gene expression during a bacterial developmental program requires DivIVA. *PLoS Genetics* **10**:e1004526 doi: [10.1371/journal.pgen.1004526](https://doi.org/10.1371/journal.pgen.1004526)
- Feucht A, Abbotts L, Errington J. 2002. The cell differentiation protein SpoIIIE contains a regulatory site that controls its phosphatase activity in response to asymmetric septation. *Molecular Microbiology* **45**:1119–1130. doi: [10.1046/j.1365-2958.2002.03082.x](https://doi.org/10.1046/j.1365-2958.2002.03082.x)
- Fujita M, Losick R. 2003. The master regulator for entry into sporulation in *Bacillus subtilis* becomes a cell-specific transcription factor after asymmetric division. *Genes & Development* **17**:1166–1174. doi: [10.1101/gad.1078303](https://doi.org/10.1101/gad.1078303)
- Fujita M. 2000. Temporal and selective association of multiple sigma factors with RNA polymerase during sporulation in *Bacillus subtilis*. *Genes to Cells : Devoted to Molecular & Cellular Mechanisms* **5**:79–88. doi: [10.1046/j.1365-2443.2000.00307.x](https://doi.org/10.1046/j.1365-2443.2000.00307.x)
- Gao T, Furnari F, Newton AC. 2005. PHLPP: a phosphatase that directly dephosphorylates akt, promotes apoptosis, and suppresses tumor growth. *Molecular Cell* **18**:13–24. doi: [10.1016/j.molcel.2005.03.008](https://doi.org/10.1016/j.molcel.2005.03.008)
- Gholamhoseinian A, Piggot PJ. 1989. Timing of spoII gene expression relative to septum formation during sporulation of *Bacillus subtilis*. *Journal of Bacteriology* **171**:5747–5749.
- Gottesman S. 2003. Proteolysis in bacterial regulatory circuits. *Annual Review of Cell and Developmental Biology* **19**:565–587.
- Handler AA, Lim JE, Losick R. 2008. Peptide inhibitor of cytokinesis during sporulation in *Bacillus subtilis*. *Molecular Microbiology* **68**:588–599. doi: [10.1111/j.1365-2958.2008.06173.x](https://doi.org/10.1111/j.1365-2958.2008.06173.x)
- Harwood CR, Cutting SM. eds. 1990. *Molecular Biological Methods for Bacillus*. Chichester:Wiley-Blackwell. 1–308.
- Herman C, Prakash S, Lu CZ, Matouschek A, Gross CA. 2003. Lack of a robust unfoldase activity confers a unique level of substrate specificity to the universal AAA protease FtsH. *Molecular Cell* **11**:659–669. doi: [10.1016/S1097-2765\(03\)00068-6](https://doi.org/10.1016/S1097-2765(03)00068-6)
- Hilbert DW, Piggot PJ. 2003. Novel spoIIIE mutation that causes uncompartimentalized sigmaF activation in *Bacillus subtilis*. *Journal of Bacteriology* **185**:1590–1598. doi: [10.1128/JB.185.5.1590-1598.2003](https://doi.org/10.1128/JB.185.5.1590-1598.2003)
- Horvitz HR, Herskowitz I. 1992. Mechanisms of asymmetric cell division: two bs or not two bs, that is the question. *Cell* **68**:237–255. doi: [10.1016/0092-8674\(92\)90468-R](https://doi.org/10.1016/0092-8674(92)90468-R)
- Iniesta AA, Shapiro L. 2008. A bacterial control circuit integrates polar localization and proteolysis of key regulatory proteins with a phospho-signaling cascade. *Proceedings of the National Academy of Sciences of the United States of America* **105**:16602–16607. doi: [10.1073/pnas.0808807105](https://doi.org/10.1073/pnas.0808807105)
- Kuwada NJ, Traxler B, Wiggins PA. 2015. Genome-scale quantitative characterization of bacterial protein localization dynamics throughout the cell cycle. *Molecular Microbiology* **95**:64–79. doi: [10.1111/mmi.12841](https://doi.org/10.1111/mmi.12841)
- Le AT, Schumann W. 2009. The SpoOE phosphatase of *Bacillus subtilis* is a substrate of the FtsH metalloprotease. *Microbiology* **155**:1122–1132. doi: [10.1099/mic.0.024182-0](https://doi.org/10.1099/mic.0.024182-0)
- Lenarcic R, Halbedel S, Visser L, Shaw M, Wu LJ, Errington J, Marenduzzo D, Hamoen LW. 2009. Localisation of DivIVA by targeting to negatively curved membranes. *The EMBO Journal* **28**:2272–2282. doi: [10.1038/emboj.2009.129](https://doi.org/10.1038/emboj.2009.129)
- Levdikov VM, Blagova EV, Rawlings AE, Jameson K, Tunaley J, Hart DJ, Barak I, Wilkinson AJ. 2012. Structure of the phosphatase domain of the cell fate determinant SpoIIIE from *Bacillus subtilis*. *Journal of Molecular Biology* **415**:343–358. doi: [10.1016/j.jmb.2011.11.017](https://doi.org/10.1016/j.jmb.2011.11.017)
- Levin PA, Losick R. 1994. Characterization of a cell division gene from *Bacillus subtilis* that is required for vegetative and sporulation septum formation. *Journal of Bacteriology* **176**:1451–1459.

- Lucet I**, Feucht A, Yudkin MD, Errington J. 2000. Direct interaction between the cell division protein FtsZ and the cell differentiation protein SpoII<sub>E</sub>. *The EMBO Journal* **19**:1467–1475. doi: [10.1093/emboj/19.7.1467](https://doi.org/10.1093/emboj/19.7.1467)
- Margolis P**, Driks A, Losick R. 1991. Establishment of cell type by compartmentalized activation of a transcription factor. *Science* **254**:562–565. doi: [10.1126/science.1948031](https://doi.org/10.1126/science.1948031)
- Min KT**, Hilditch CM, Diederich B, Errington J, Yudkin MD. 1993. Sigma F, the first compartment-specific transcription factor of *B. subtilis*, is regulated by an anti-sigma factor that is also a protein kinase. *Cell* **74**:735–742. doi: [10.1016/0092-8674\(93\)90520-Z](https://doi.org/10.1016/0092-8674(93)90520-Z)
- Neumüller RA**, Knoblich JA. 2009. Dividing cellular asymmetry: asymmetric cell division and its implications for stem cells and cancer. *Genes & Development* **23**:2675–2699. doi: [10.1101/gad.1850809](https://doi.org/10.1101/gad.1850809)
- Piggot PJ**, Coote JG. 1976. Genetic aspects of bacterial endospore formation. *Bacteriological Reviews* **40**:908–962.
- Ramamurthi KS**, Losick R. 2009. Negative membrane curvature as a cue for subcellular localization of a bacterial protein. *Proceedings of the National Academy of Sciences of the United States of America* **106**:13541–13545. doi: [10.1073/pnas.0906851106](https://doi.org/10.1073/pnas.0906851106)
- Rudner DZ**, Losick R. 2002. A sporulation membrane protein tethers the pro-sigma k processing enzyme to its inhibitor and dictates its subcellular localization. *Genes & Development* **16**:1007–1018. doi: [10.1101/gad.977702](https://doi.org/10.1101/gad.977702)
- Schuck P**. 2000. Size-distribution analysis of macromolecules by sedimentation velocity ultracentrifugation and lamm equation modeling. *Biophysical Journal* **78**:1606–1619. doi: [10.1016/S0006-3495\(00\)76713-0](https://doi.org/10.1016/S0006-3495(00)76713-0)
- Sliusarenko O**, Heinritz J, Emonet T, Jacobs-Wagner C. 2011. High-throughput, subpixel precision analysis of bacterial morphogenesis and intracellular spatio-temporal dynamics. *Molecular Microbiology* **80**:612–627. doi: [10.1111/j.1365-2958.2011.07579.x](https://doi.org/10.1111/j.1365-2958.2011.07579.x)
- Stragier P**, Losick R. 1996. Molecular genetics of sportulation in *Bacillus subtilis*. *Annual Review of Genetics* **30**:297–341.
- Su J**, Schlicker C, Forchhammer K. 2011. A third metal is required for catalytic activity of the signal-transducing protein phosphatase m tPphA. *Journal of Biological Chemistry* **286**:13481–13488. doi: [10.1074/jbc.M109.036467](https://doi.org/10.1074/jbc.M109.036467)
- Thompson LS**, Beech PL, Real G, Henriques AO, Harry EJ. 2006. Requirement for the cell division protein DivIB in polar cell division and engulfment during sporulation in bacillus subtilis. *Journal of Bacteriology* **188**:7677–7685. doi: [10.1128/JB.01072-06](https://doi.org/10.1128/JB.01072-06)
- Veening JW**, Stewart EJ, Berngruber TW, Taddei F, Kuipers OP, Hamoen LW. 2008. Bet-hedging and epigenetic inheritance in bacterial cell development. *Proceedings of the National Academy of Sciences of the United States of America* **105**:4393–4398. doi: [10.1073/pnas.0700463105](https://doi.org/10.1073/pnas.0700463105)
- Wu LJ**, Feucht A, Errington J. 1998. Prespore-specific gene expression in bacillus subtilis is driven by sequestration of SpoII<sub>E</sub> phosphatase to the prespore side of the asymmetric septum. *Genes & Development* **12**:1371–1380. doi: [10.1101/gad.12.9.1371](https://doi.org/10.1101/gad.12.9.1371)